

# Study on Superabsorbent Composites. XVIII. Preparation, Characterization, and Property Evaluation of Poly(acrylic acid-co-acrylamide)/Organomontmorillonite/Sodium Humate Superabsorbent Composites

Yian Zheng, Ai Qin Wang

Center of Ecomaterials and Green Chemistry, Lanzhou Institute of Chemical Physics, Chinese Academy of Sciences, Lanzhou 730000, People's Republic of China

Received 4 March 2007; accepted 2 October 2007

DOI 10.1002/app.27439

Published online 27 December 2007 in Wiley InterScience (www.interscience.wiley.com).

**ABSTRACT:** A series of novel multifunctional poly (acrylic acid-co-acrylamide) (PAA-AM)/organomontmorillonite (O-MMT)/sodium humate (SH) superabsorbent composites were synthesized by the graft copolymerization reaction of partially neutralized acrylic acid and acrylamide on O-MMT micropowder and SH with *N,N'*-methylene bisacrylamide as a crosslinker and ammonium persulfate as an initiator in an aqueous solution. The superabsorbent composites were characterized by means of Fourier transform infrared spectroscopy, X-ray diffraction, scanning electron microscopy, and thermogravimetric analysis. The effect of the relative weight ratio of SH to O-MMT on the water absorbency was studied, and the results indicated that the best water absorbency of 591 g/g in distilled water was obtained when an O-MMT content of 20 wt % and an SH content of 30 wt % were incorporated. The

superabsorbent composite possessed a good capacity for water retention; even after 30 days, 24.4 wt % of water could still be saved by the sand soil containing 1.0 wt % superabsorbent composite. The results from this study show that the water absorbency of a superabsorbent composite is improved by the simultaneous introduction of O-MMT and SH into a PAA-AM network in comparison with the incorporation of only O-MMT or SH. Also, in comparison with PAA-AM/MMT/SH, an appropriate amount of O-MMT can benefit the developed composites with respect to their water absorbency, salt resistance, and capacity for water retention in sand soil. © 2007 Wiley Periodicals, Inc. *J Appl Polym Sci* 108: 211–219, 2008

**Key words:** composites; graft copolymers; hydrogels; hydrophilic polymers; swelling

## INTRODUCTION

Superabsorbent polymers are water-insoluble and loosely crosslinked hydrophilic polymers. Because of their excellent characteristics, superabsorbents not only are widely used in traditional fields including hygienic products, horticulture, and agriculture<sup>1–3</sup> but also are being introduced into some promising fields, such as biotechnological devices, drug-delivery systems, tissue engineering, and immobilization of enzymes.<sup>6–11</sup> Along with the development of superabsorbents, numerous studies have been devoted to the discovery of clay-based superabsorbent composites and polymer matrix/organically modified clay systems in which wide clay dispersion at least and clay exfoliation at best are obtained.<sup>12–20</sup>

Correspondence to: A. Wang (aqwang@lzb.ac.cn).

Contract grant sponsor: West Light Foundation and Western Action Project of the Chinese Academy of Sciences; contract grant number: KGCX2-YW-501.

Contract grant sponsor: 863 Project of the Ministry of Science and Technology, People's Republic of China; contract grant number: 2006AA03Z0454.

Some of the most important applications of superabsorbent polymers are agricultural and horticultural, and an optimized combination of a superabsorbent with a slow-release fertilizer is an effective way to develop water-saving cultivation and ecological and environmental construction. In this field, to avoid or reduce the loss of fertilizer containing nitrogen atoms, Liu and coworkers<sup>21,22</sup> reported the preparation and properties of superabsorbent composites with slow-release behaviors of urea, and significant advantages were obtained. Sodium humate (SH), consisting of multifunctional aliphatic components and aromatic constituents, contains a large number of functional groups (e.g., carboxylates and phenolic hydroxyls),<sup>23</sup> and it has been described as the most important component of healthy, fertile soil.<sup>24</sup> In our previous study, a superabsorbent with high water absorbency was obtained by the introduction of SH into a poly(acrylic acid-co-acrylamide) (PAA-AM) system.<sup>25</sup>

Up to now, montmorillonite (MMT)-based superabsorbent composites have been reported by other researchers,<sup>26</sup> but an effective combination of MMT or organomontmorillonite (O-MMT) and SH in a superabsorbent composite has not been reported.

Consequently, on the basis of our previous studies on superabsorbent composites,<sup>27–29</sup> in this study, a series of novel multifunctional PAA-AM/O-MMT/SH composites were prepared by the simultaneous introduction of O-MMT and SH into the PAA-AM polymeric network, and the composites were characterized by means of Fourier transform infrared (FTIR), X-ray diffraction (XRD), scanning electron microscopy (SEM), and thermogravimetric analysis (TGA). The swelling behaviors in various cationic saline solutions, the swelling kinetics in distilled water, and the capacity for water retention of the developed composites in sand soil were investigated and evaluated. For comparison, PAA-AM/MMT/SH composites were involved, and their properties were also systematically studied.

## EXPERIMENTAL

### Materials

Hexadecyltrimethyl ammonium bromide (HDTMABr; analytical grade; Shanghai Shanpu Chemical Reagent Factory, Shanghai, China) was used directly as received. Acrylic acid (AA; chemically pure; Shanghai Wulian Chemical Factory, Shanghai, China) was distilled under reduced pressure before use. Acrylamide (AM; analytical grade; Beijing Chemical Factory, Beijing, China) was purified by recrystallization from benzene. The initiator, ammonium persulfate (APS; analytical grade; Tianjin Chemical Reagent Factory, Tianjin, China), was recrystallized from water. The crosslinker, *N,N'*-methylene bisacrylamide (MBA; chemically pure; Shanghai Chemical Reagent Factory, Shanghai, China), was used as purchased. SH (Shuanglong, Ltd., Xinjiang, China) and calcium montmorillonite (Ca-MMT, Longfeng Montmorillonite Co., Shandong, China) were industrial-grade and were milled through a 320-mesh screen before use. Other reagents were all analytical-grade, and all solutions were prepared with distilled water.

### Preparation of O-MMT

O-MMT was synthesized according to the following procedure. HDTMABr with a cation-exchange capacity (CEC) for MMT equal to 0.25, 0.50, 1.0, 2.0, or 3.0 was dissolved in 100 mL of distilled water, and then 4.0 g of MMT was slowly added. The reaction mixtures were stirred continuously at room temperature for 8 h to form the organomodified MMT. The mixture was filtered and washed several times with distilled water until no bromide ion was detected with a  $\text{AgNO}_3$  solution (0.1M). The product was dried in an air oven at 70°C to a constant weight and ground to a 320-mesh size.

### Preparation of the PAA-AM/O-MMT/SH superabsorbent composites

A series of superabsorbent composites with different weight ratios of SH to O-MMT were prepared as follows. Under a nitrogen atmosphere, 3.55 g of AM and 4.32 g of AA with a 70% neutralization degree (neutralized with a 4M sodium hydroxide solution in an ice bath) were introduced into 36 mL of distilled water in a 250-mL, four-necked flask equipped with a stirrer, a condenser, a thermometer, and a nitrogen line. The crosslinker MBA (15.9 mg) was added to the mixture solution, and then an appropriate weight ratio of SH to O-MMT was dispersed. After stirring for 30 min, the mixed solution was heated to 50°C gradually, and then the initiator APS (95.6 mg) was put into the flask. The solution was stirred at 80°C for 3 h to complete the polymerization reaction. During the polymerization reaction, the total weight ratio of SH and O-MMT was constant: 50 wt %. A general reaction mechanism for the final three-dimensional network of the superabsorbent composite is proposed as follows.<sup>9</sup> Under heating, the thermal dissociation initiator APS is decomposed to produce a sulfate anion radical. Then, the resulting anion radical abstracts hydrogen from one of the functional groups (e.g.,  $-\text{COOH}$  and  $-\text{OH}$ ) existing in MMT and SH to form the corresponding radical. Consequently, these macroradicals initiate the grafting of the monomers onto MMT and SH, leading to a graft copolymer. Simultaneously, the crosslinking reaction is carried out in the presence of MBA; thus, a three-dimensional network is achieved. After polymerization, the resulting product was dried at 70°C to a constant weight. The dark products were milled, and all samples used for testing had a particle size in the range of 40–80 mesh.

The procedure for the preparation of PAA-AM, PAA-AM/O-MMT, PAA-AM/SH, and PAA-AM/MMT/SH was similar to that for the preparation of the PAA-AM/O-MMT/SH superabsorbent composite, except without the addition of O-MMT and/or SH, or MMT was used instead of O-MMT.

### Characterization of the superabsorbent composite

FTIR spectra were recorded on a Thermo Nicolet Nexus FTIR apparatus (Thermo Nicolet Corporation, Madison, WI) in the range of 4000–400  $\text{cm}^{-1}$  with KBr pellets. XRD patterns were obtained with an X'Pert Pro diffractometer (Cu  $\text{K}\alpha$  radiation, 40 kV, 30 mA) (Philips, Almelo, Netherlands). SEM studies were carried out with a JSM-5600LV SEM instrument (JEOL, Ltd., Tokyo, Japan) after the sample was coated with a gold film. Thermal stability studies were performed on a PerkinElmer TGA-7 thermogravimetric analyzer (Perkin Elmer Cetus Instruments,

Norwalk, CT) at a heating rate of 10°C/min in nitrogen (50 mL/min) from room temperature to 800°C.

### Measurement of the water absorbency and swelling behavior

A series of weighed dried samples were immersed in excess distilled water or various saline solutions at room temperature until swelling equilibrium was achieved. Swollen samples were then separated from unabsorbed water by filtration with a 100-mesh stainless screen and suspension for 10 min. The equilibrium swelling ratio ( $Q$ ) was calculated with the following equation:

$$Q = (m_2 - m_1)/m_1 \quad (1)$$

where  $m_1$  and  $m_2$  are the weights of the dry sample and swollen sample, respectively.  $Q$  was calculated as grams of water per gram of sample.

### Determination of the swelling kinetics

The swelling rate for the superabsorbent composite was measured as follows. A series of weighed dried samples (50 mg) were immersed in excess distilled water at room temperature for different times and then separated from unabsorbed water by filtration with a 100-mesh stainless screen and suspension for 10 min. The water absorbency for different times could then be calculated according to eq. (1).

### Measurement of the water retention properties in sand soil

In this experiment, 0.1, 0.5, or 1.0 wt % superabsorbent composite (with respect to the mass of the sand soil) was well mixed in cups with 200 g of sand soil. Tap water (60 g) was slowly added to the cups, and the cups were weighed at different set intervals. This measurement was carried out at room temperature. The practical water retention capacity of the superabsorbent composite could then be obtained. A compared (controlled) experiment without the superabsorbent composite was also performed as a reference.

## RESULTS AND DISCUSSION

### FTIR analysis

Figure 1 shows the FTIR spectra of Ca-MMT, Ca-MMT with a 0.25 CEC, Ca-MMT with a 0.5 CEC, Ca-MMT with a 1.0 CEC, and Ca-MMT with a 2.0 CEC. The appearance of strong absorption bands at 2923, 2851, and 1475  $\text{cm}^{-1}$  can be ascribed to the characteristic peaks of HDTMABr, an indication of

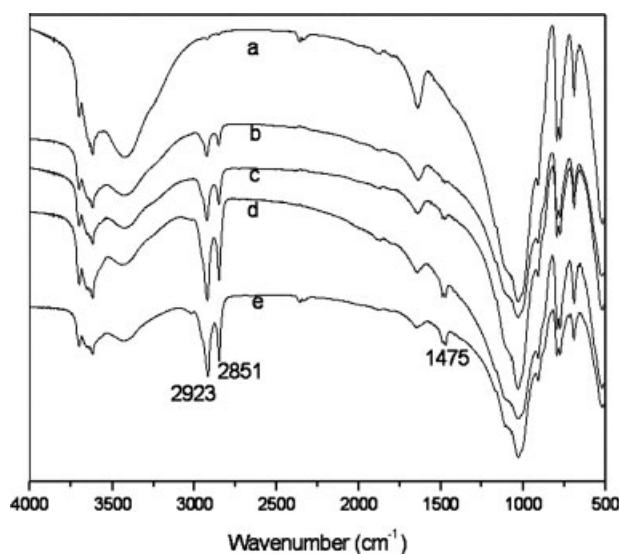


**Figure 1** FTIR spectra of (a) Ca-MMT, (b) MMT-0.25 CEC, (c) MMT-0.5 CEC, (d) MMT-1.0 CEC, and (e) MMT-2.0 CEC.

the organization of MMT. In addition, the absorption bands increase with an increase in CEC of MMT. A careful study to compare the infrared spectra of PAA-AM/O-MMT/SH and SH, PAA-AM, and O-MMT has also been performed, as shown in Figure 2. In the infrared spectrum of PAA-AM/O-MMT/SH, the appearance of the absorption bands at 1652, 1456, and 1409 ( $\text{cm}^{-1}$ ) (the characteristic absorption bands of  $-\text{CONH}_2$ ), 1570 ( $\text{cm}^{-1}$ ) ( $-\text{COO}^-$  asymmetric stretching), and 1040, 519, and 461  $\text{cm}^{-1}$  (the characteristic absorption bands of  $\text{Si}-\text{O}-\text{Si}$  and  $\text{Si}-\text{O}-\text{R}^{3+}$  in Ca-MMT<sup>29</sup>) provides direct evidence for the interaction between O-MMT, SH, and PAA-AM. After polymerization, the absorption bands of SH at 1713  $\text{cm}^{-1}$  ( $\text{C}=\text{O}$  stretching of carboxylic group) as well as 3621 (vibration absorption of  $-\text{OH}$  in Ca-MMT) and 912  $\text{cm}^{-1}$  ( $\text{Al}-\text{OH}$ ) are absent in the spectrum of the PAA-AM/O-MMT/SH polymeric network. A new absorption band lying at 1274  $\text{cm}^{-1}$ , attributable to the ethereal oxygen attached to an aromatic ring<sup>30</sup> (the aromatic ring is ascribed to the existence of SH), has emerged. Therefore, it is concluded that some chemical reactions, such as the graft reaction of SH, occur between PAA-AM, O-MMT, and SH during the polymerization process.

### XRD patterns

XRD patterns of Ca-MMT, O-MMT, and the PAA-AM/O-MMT/SH composite are displayed in Figure 3. A typical diffraction peak of Ca-MMT at  $2\theta = 5.92^\circ$ , which corresponds to a basal spacing of 1.49 nm, is clear in Figure 3(a). After organization with HDTMABr, this characteristic peak remains unchange-

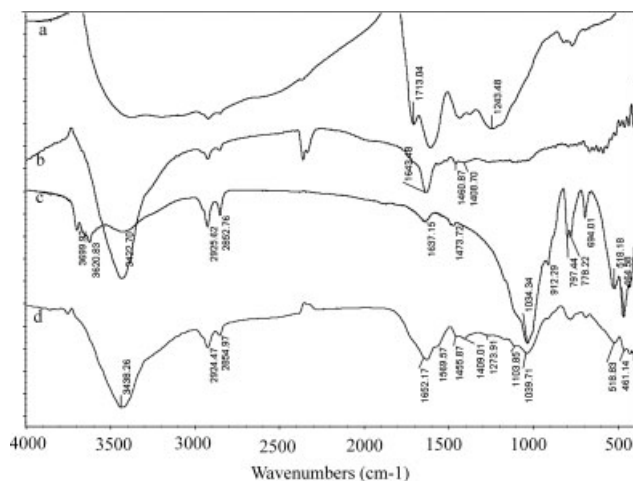


**Figure 2** FTIR spectra of (a) SH, (b) PAA-AM, (c) MMT-0.5 CEC, and (d) PAA-AM/O-MMT/SH. The sum of SH and O-MMT is 50 wt %. The weight ratio of SH to O-MMT is 3 : 2.

able, indicating that HDTMABr is just adsorbed on the surface of MMT during the cation-exchange process without destroying the crystalline structure. The absence of this characteristic diffraction peak in PAA-AM/O-MMT/SH suggests that the clay platelets of O-MMT are exfoliated and then are thoroughly dispersed in the polymer matrix, forming a composite structure. In comparison with sodium montmorillonite (Na-MMT), the intercalated structure is not formed during the reaction between Ca-MMT and HDTMABr, likely because of its larger interlayer distance ( $d_{001} = 1.49$  nm) compared with that of Na-MMT ( $d_{001} = 1.23$  nm<sup>20</sup>).

### Morphology

The micrographs of PAA-AM/MMT/SH and PAA-AM/O-MMT/SH are shown in Figure 4. In lower magnification SEM, PAA-AM/MMT/SH and PAA-AM/O-MMT/SH present similar surface morphologies [Fig. 4(a,c)]; no obvious differences can be observed. However, in higher magnification SEM, the morphology of PAA-AM/O-MMT/SH [Fig. 4(d)] is different from that of PAA-AM/MMT/SH [Fig. 4(b)]. PAA-AM/O-MMT/SH shows an incompact, finely dispersed structure, whereas PAA-AM/MMT/SH exhibits a tight, smooth surface. This different surface structure would affect the water absorbency behavior.<sup>14,20</sup>

Apart from the surface analysis for PAA-AM/O-MMT/SH and PAA-AM/MMT/SH, for the same samples, micrographs for the cross-sectional areas have also been taken [Fig. 4(e,f)]. For both PAA-AM/MMT/SH and PAA-AM/O-MMT/SH, the cross-sectional areas show similar tight morphologies compared with the surfaces of the corresponding

composites, except for some protuberances found in the cross-sectional area of PAA-AM/O-MMT/SH. Therefore, it can be concluded that the developed composite is uniform, and no obvious differences in the entire micrographs have been observed.

### TGA

TGA curves of PAA-AM, PAA-AM/MMT/SH, and PAA-AM/O-MMT/SH superabsorbent composites are well presented in Figure 5. These samples showed a similar loss at 25–200°C, an indication of a loss of moisture present in them. The major exothermic peak for PAA-AM was located at 423°C, whereas for PAA-AM/MMT/SH and PAA-AM/O-MMT/SH, sharp weight losses at 495 and 490°C were observed. Furthermore, the PAA-AM/O-MMT (or MMT)/SH polymeric network can also provide a lower weight loss over the temperature range investigated. The improved thermal stability can be ascribed to the barrier effect of MMT.<sup>14</sup> MMT is a layered structure, and small molecules generated during the thermal decomposition process cannot permeate, and thus have to bypass, MMT layers.<sup>31</sup> It is worth pointing out that the thermal stability of PAA-AM/MMT/SH is slightly higher than that of PAA-AM/O-MMT/SH with the same clay and SH contents. The lower thermal stability of PAA-AM/O-MMT/SH may have arisen from the presence of HDTMABr species.<sup>32</sup>

### Effect of the organization of MMT on the water absorbency

The effect of the organization of MMT on the water absorbency of the superabsorbent composite was

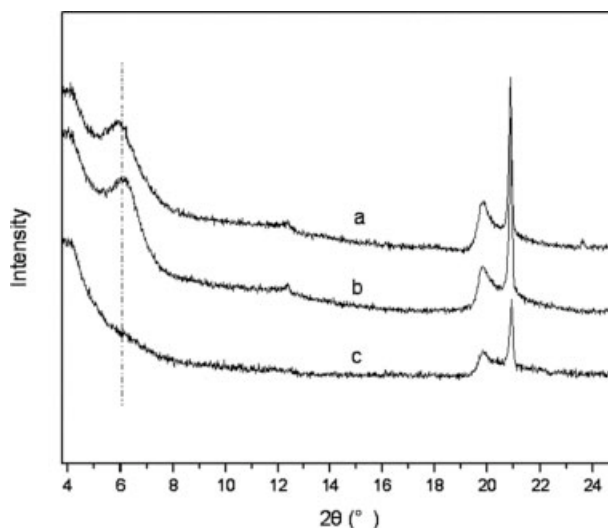


**Figure 3** XRD powder patterns for (a) Ca-MMT, (b) MMT-0.5 CEC, and (c) PAA-AM/O-MMT/SH. The sum of SH and O-MMT is 50 wt %. The weight ratio of SH to O-MMT is 3 : 2.

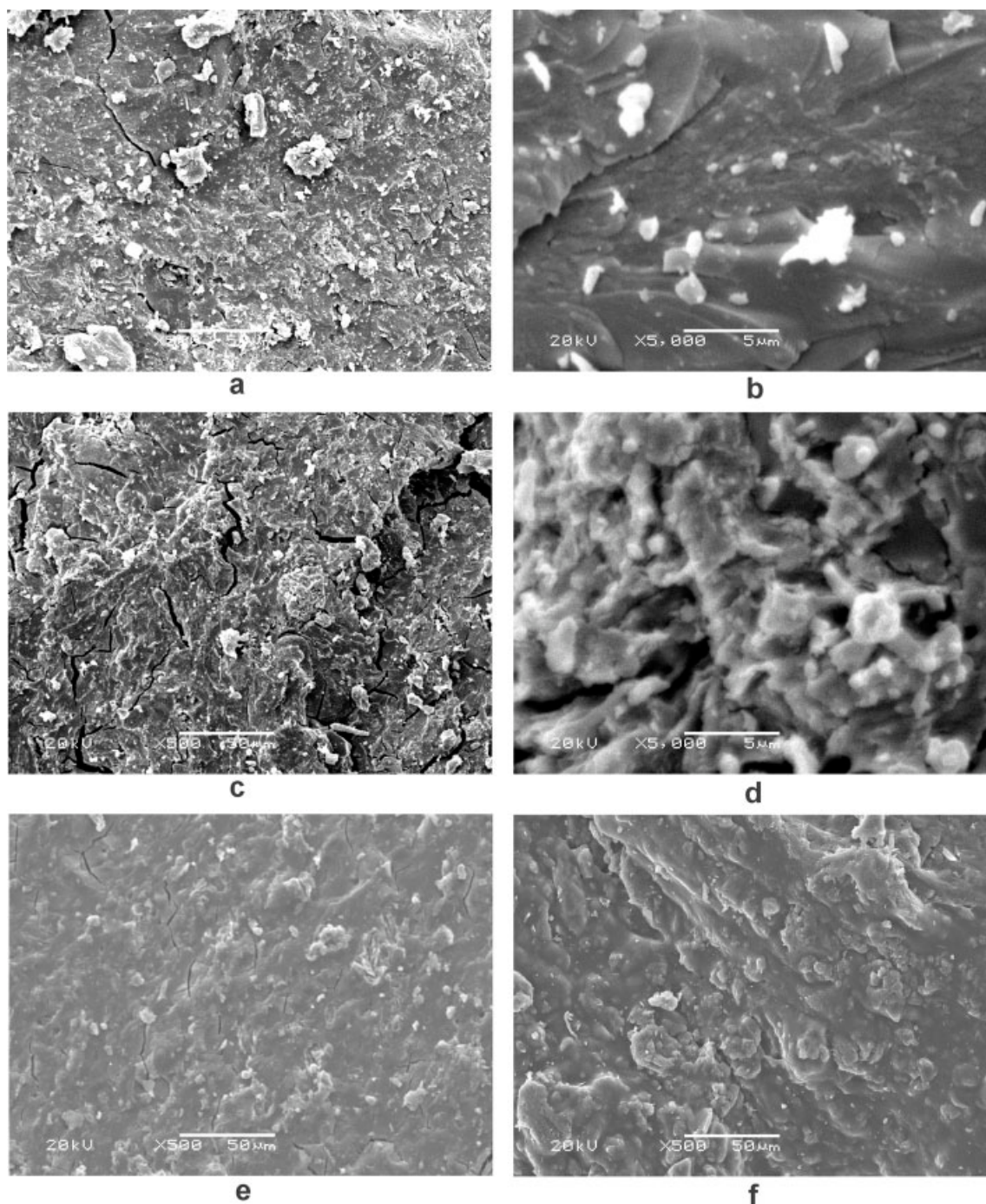


**Figure 4** SEM images of (a) PAA-AM/MMT/SH at a lower magnification, (b) PAA-AM/MMT/SH at a higher magnification, (c) PAA-AM/O-MMT/SH at a lower magnification, (d) PAA-AM/O-MMT/SH at a higher magnification, (e) the cross-sectional area of PAA-AM/MMT/SH, and (f) the cross-sectional area of PAA-AM/O-MMT/SH. The sum of SH and O-MMT or MMT is 50 wt %. The weight ratio of SH to O-MMT or MMT is 3 : 2.

investigated, as shown in Figure 6. It is clear that with an increasing degree of organification (from 0.25 CEC to 1.0 CEC), no significant differences in the water absorbency can be observed. However, with a further increase in CEC from 1.0 to 3.0, the water absorbency of the superabsorbent composite in distilled water decreased remarkably. This is due

to the fact that the effect of O-MMT on the improvement of the PAA-AM/O-MMT/SH polymeric network was not evident when a lower CEC of MMT was realized. However, too high a CEC of MMT leads to too much hydrophobic region, and the hydrophilicity of the composite decreases; this results in the shrinkage of the corresponding super-

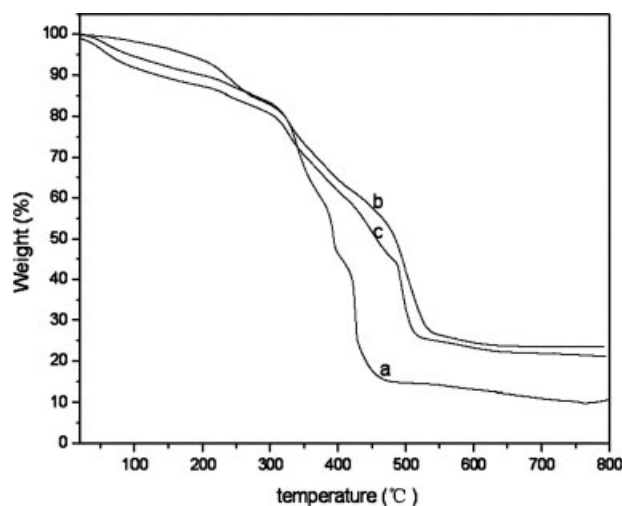


**Figure 5** TGA curves of (a) PAA-AM, (b) PAA-AM/MMT/SH, and (c) PAA-AM/O-MMT/SH. The sum of SH and O-MMT or MMT is 50 wt %. The weight ratio of SH to O-MMT or MMT is 3 : 2.

absorbent composite. This behavior is similar to that seen in our previous study about attapulgite.<sup>32</sup> This means that an appropriate organization of MMT is required for an excellent superabsorbent composite. The water absorbency in 0.9 wt % NaCl shows a similar tendency. For further study, a 0.5 CEC of MMT was recommended.

#### Effect of the weight ratio of SH to O-MMT on the water absorbency

With the total weight ratio of SH to O-MMT or MMT fixed at 50 wt %, the effect of the relative weight ratio of SH to O-MMT or MMT on the water absorbency was investigated, as shown in Figure 7. Compared with the single introduction of O-MMT

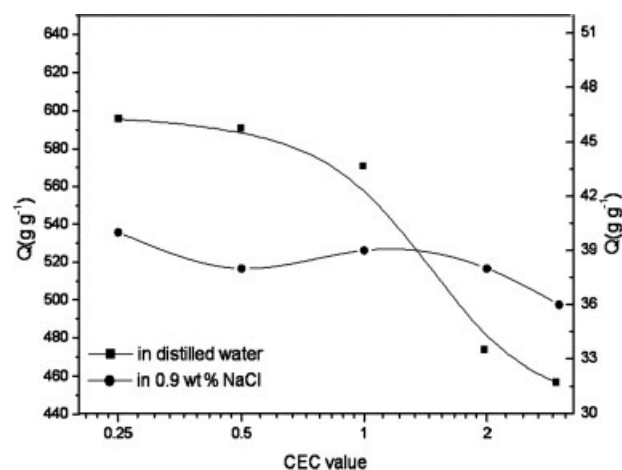


**Figure 6** Water absorbency ( $Q$ ) for the superabsorbent composites as a function of the organization of MMT. The sum of SH and O-MMT is 50 wt %. The weight ratio of SH to O-MMT is 3 : 2.

(365 g/g) or SH (425 g/g), the simultaneous incorporation of O-MMT and SH could provide the best water absorbency. The superabsorbent composite with 30 wt % SH and 20 wt % O-MMT provided the optimum water absorbency of 591 g/g in distilled water. This may have been due to the cooperative effects of O-MMT and SH, and a similar result was obtained in our previous study on attapulgite.<sup>29</sup> In comparison with PAA-AM/MMT/SH, with the content of SH increasing from 0 to 60 wt % (between SH and MMT), no obvious differences in the water absorbency were observed for PAA-AM/O-MMT/SH. However, a further increase in the SH content, such as a weight ratio of 4:1 (SH to O-MMT), was followed by a remarkable improvement in the water absorbency for the composite. Therefore, the weight ratio of SH to O-MMT of 4 : 1 was chosen for the swelling study.

#### Swelling behavior in various cationic saline solutions

In this section, the swelling behaviors of PAA-AM/O-MMT/SH in various saline solutions are examined. Among the factors influencing the water absorbency of superabsorbent composites, the kind of cation is the key factor.<sup>33</sup> The swelling behaviors of the superabsorbent composite in three cationic saline solutions (NaCl, CaCl<sub>2</sub>, and FeCl<sub>3</sub>) were systematically investigated, and the results are shown in Figure 8. The water absorbency at the same salt concentration has the following order: NaCl > CaCl<sub>2</sub> > FeCl<sub>3</sub>. This is due to the fact that multivalent Ca<sup>2+</sup> and Fe<sup>3+</sup> ions may crosslink the gel with the carboxylate groups on adjacent chains or chain segments of

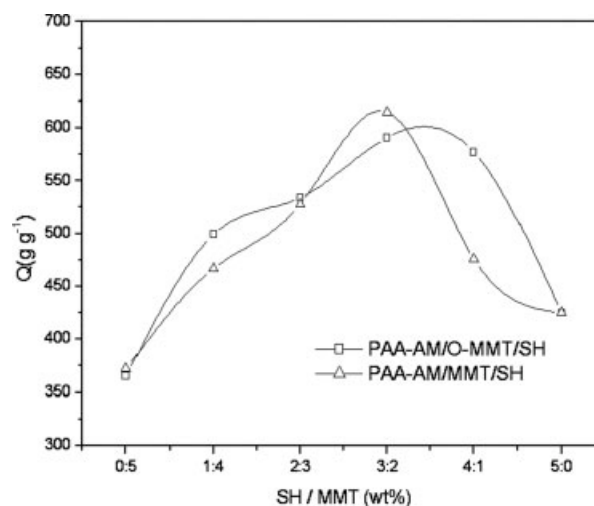


**Figure 7** Effect of the relative weight ratio of SH to O-MMT or MMT on the water absorbency ( $Q$ ) for the superabsorbent composites. The sum of SH and MMT is 50 wt %.

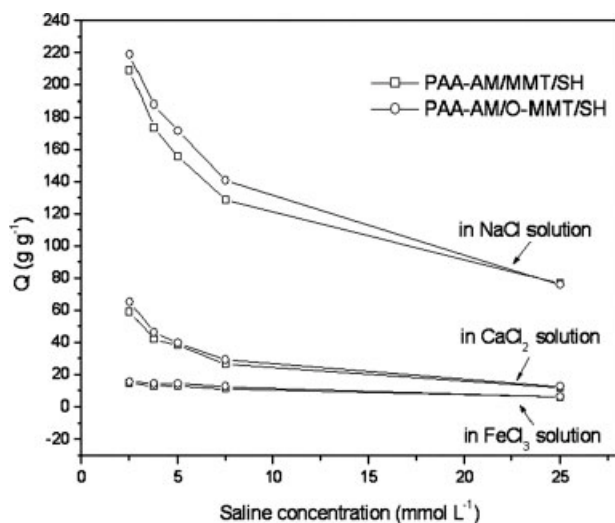


**Figure 8** Equilibrium water absorbency ( $Q$ ) of the superabsorbent composites in NaCl, CaCl<sub>2</sub>, and FeCl<sub>3</sub> solutions with various concentrations. The sum of SH and O-MMT or MMT is 50 wt %. The weight ratio of SH to O-MMT or MMT is 4 : 1.

the copolymer via the formation of a coordination bond.<sup>33</sup> Consequently, the crosslink density of the network increases, leading the water absorbency to decrease. In addition, the water absorbency for these superabsorbent composites decreases with an increase in the ionic strength of saline solutions. This salt effect is clearly evidenced as a result of the osmotic pressure difference between the internal solution in the gel and the external solution due to different ion concentrations.<sup>34,35</sup> In addition, the PAA-AM/O-MMT/SH composite shows a higher water absorbency in all cationic saline solutions with the same concentration in comparison with PAA-AM/MMT/SH. This tendency of water absorbency is similar to that in distilled water. This result indicates that PAA-AM/O-MMT/SH possesses good salt-resistance properties.

The relationship between the water absorbency of the composite and the ionic strength of external NaCl solutions was investigated, as shown in Figure 9. Hermans<sup>36</sup> suggested that the relationship between the swelling ability of a superabsorbent composite and the ionic strengths of the external solution agreed with the following equation:

$$Q_{eq}^{5/3} = A + Bi^2/I \quad (2)$$

where  $Q_{eq}$  is the saturated water absorbency,  $i$  is the charge density on the gel,  $I$  is the ionic strength of the external solution, and  $A$  and  $B$  are empirical parameters. By plotting  $Q_{eq}^{5/3}$  against the reciprocal of  $I$ , as indicated in Figure 9, we have obtained an approximately linear relationship within the range of  $I$  studied. This is explained by the fact that the

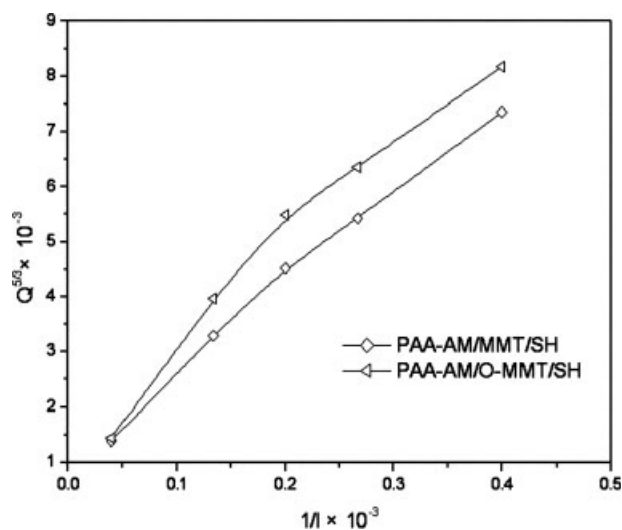


**Figure 9** Relationship between the water absorbency ( $Q$ ) and ionic strength ( $I$ ) of external NaCl solutions. The sum of SH and O-MMT or MMT is 50 wt %. The weight ratio of SH to O-MMT or MMT is 4 : 1.

elastic force of the polymeric network interferes with the swelling force. Similar results were obtained in our previous study of a polyacrylamide/attapulgite system.<sup>37</sup>

### Swelling kinetics of the superabsorbent composites

The superabsorbent composite, characterized by its swelling kinetics, is shown in Figure 10. The swelling rate underwent a great change in the first 30 min, and the water absorbency of PAA-AM/SH/MMT reached 363 g/g within 30 min, whereas 449 g/g was achieved for the PAA-AM/O-MMT/SH

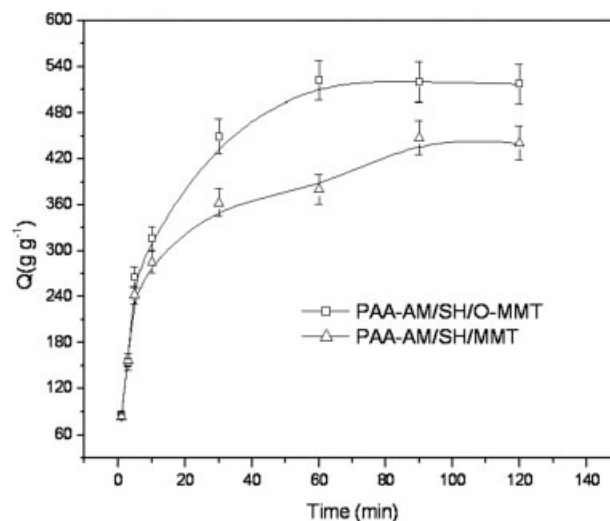


**Figure 10** Swelling kinetics of the superabsorbent composites in distilled water. The sum of SH and O-MMT or MMT is 50 wt %. The weight ratio of SH to O-MMT or MMT is 4 : 1.

composite. After 30 min, the curves of the swelling rate became flatter, and this indicated that the saturated water absorbency in distilled water was achieved. Saturated water absorbency for PAA-AM/O-MMT/SH was acquired within 60 min, but PAA-AM/SH/MMT required around 90 min. In comparison with the swelling kinetics of the PAA-AM/MMT/SH polymeric network, the PAA-AM/O-MMT/SH polymeric network required less time to achieve the equilibrium. The differences in the swelling rate may be attributed to different surface morphologies for the developed composite and PAA-AM/MMT/SH. As observed from Figure 4(b,d), the incompact, finely dispersed structure for the PAA-AM/O-MMT/SH polymeric network was responsible for the fast swelling rate, in comparison with the tight, smooth surface structure of the PAA-AM/MMT/SH polymeric network.

### Practical water retention in sand soil

The water retention capacity of superabsorbent composites in practical soils is more significant, as they would be applied to these fields as water-managing materials. A practical water retention test in sand soil for the PAA-AM/O-MMT/SH composite was performed and compared with that of the PAA-AM/MMT/SH composite, as shown in Figure 11. It is clear that the water retention in sand soil decreased as the time was prolonged, and the sand soil containing the PAA-AM/O-MMT/SH superabsorbent composite possessed a higher water retention capacity than the sand soil with PAA-AM/MMT/SH. After 20 days, the water retention of the compared (controlled) sample was 0.4 wt %, whereas

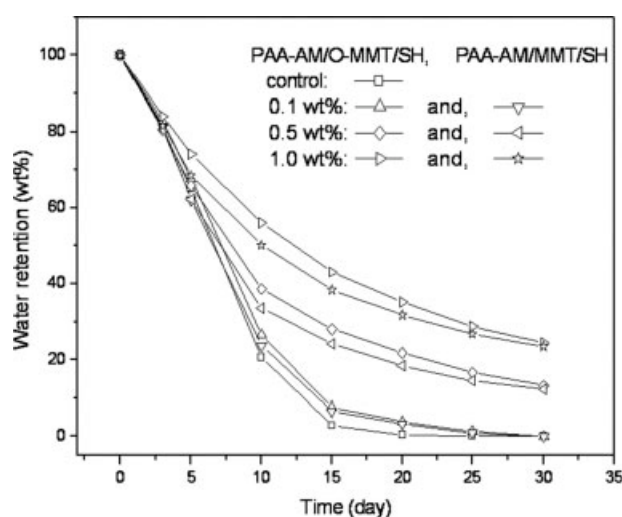


**Figure 11** Practical water retention capacities of the superabsorbent composites in sand soil. The sum of SH and O-MMT or MMT is 50 wt %. The weight ratio of SH to O-MMT or MMT is 4 : 1.

the sand soil samples containing the PAA-AM/O-MMT/SH composite at a concentration of 0.1, 0.5, or 1.0 wt % still possessed 3.8, 21.7, or 35.2 wt % of the water, respectively. Even after 30 days, 24.4 wt % of the water was still retained by the sand soil containing a 1.0 wt % concentration of the developed composite. This result indicates that the PAA-AM/O-MMT/SH superabsorbent composite can enhance the water retention capacity in sand soil. This characteristic makes it more important for practical applications, especially in arid and desert areas.

### CONCLUSIONS

A series of novel multifunctional PAA-AM/O-MMT/SH superabsorbent composites with a best water absorbency of 519 g/g in distilled water were synthesized. FTIR indicated that MMT was organified and that some reactions, including the graft reaction of SH, occurred between PAA-AM, O-MMT, and SH. SEM studies showed an incompact, finely dispersed structure of the clay particles in the PAA-AM/O-MMT/SH polymer matrix with respect to that of PAA-AM/MMT/SH. This different surface structure could affect the water absorbency behavior. The water absorbency at the same salt concentration had the following order: NaCl > CaCl<sub>2</sub> > FeCl<sub>3</sub>. The results from this study show that the water absorbency and salt-resistance properties of PAA-AM/O-MMT/SH with an appropriate amount of O-MMT are better than those of PAA-AM/MMT/SH, and the water absorbency of the composite is improved by the simultaneous introduction of O-MMT and SH into the PAA-AM network in comparison with the incorporation of only O-MMT or SH. The PAA-AM/O-MMT/SH composite possesses a good water retention capacity; even after 30 days, 24.4 wt % of the water can still be saved by sand soil containing a 1.0 wt % concentration of the superabsorbent composite.

### References

- Buchholz, F. L.; Graham, T. *Modern Superabsorbent Polymer Technology*; Wiley-VCH: New York, 1998.
- Xu, G.; Wu, G. Y.; Li, L. *Spec Petrochem* 2002, 1, 42.
- Mohan, Y. M.; Murthy, P. S. K.; Raju, K. M. *React Funct Polym* 2005, 63, 11.
- Shiga, T.; Hirose, Y.; Okada, A.; Kurauchi, T. *J Appl Polym Sci* 1992, 44, 249.
- Shiga, T.; Hirose, Y.; Okada, A.; Kurauchi, T. *J Appl Polym Sci* 1993, 47, 113.
- Stayton, P. S.; Shimoboji, T.; Long, C.; Chilkoti, A.; Chen, G.; Harris, J. M.; Hoffman, A. S. *Nature* 1995, 378, 472.
- Stile, R. A.; Burghardt, W. R.; Healy, K. E. *Macromolecules* 1999, 32, 7370.
- Takeuchi, S.; Omodaka, I. *Makromol Chem* 1993, 194, 1991.
- Pourjavadi, A.; Sadeghi, M.; Hashemi, M. M.; Hosseinzadeh, H. *e-Polymers* 2006, 57, 1.



10. Okano, T.; Bae, Y. H.; Jacobs, H.; Kim, S. W. *J Controlled Release* 1990, 11, 255.
11. Makino, K.; Hiyoshi, J.; Ohshima, H. *Colloids Surf B* 2001, 20, 341.
12. Ma, L.; Zhang, L.; Yang, J. C.; Xie, X. M. *J Appl Polym Sci* 2002, 86, 2272.
13. Lee, W. F.; Lin, G. H. *J Appl Polym Sci* 2001, 79, 1665.
14. Santiago, F.; Mucientes, A. E.; Osorio, M.; Rivera, C. *Eur Polym J* 2007, 43, 1.
15. Zhang, J.; Li, A.; Wang, A. *Carbohydr Polym* 2006, 65, 150.
16. Kabiri, K.; Zohuriaan-Mehr, M. J. *Polym Adv Technol* 2003, 14, 438.
17. Lin, J.; Wu, J.; Yang, Z.; Pu, M. *Macromol Rapid Commun* 2001, 22, 422.
18. Lee, W. F.; Chen, Y. C. *J Appl Polym Sci* 2004, 94, 2417.
19. Zheng, Y. A.; Li, P.; Zhang, J. P.; Wang, A. Q. *Eur Polym J* 2007, 43, 1691.
20. Lee, W. F.; Yang, L. G. *J Appl Polym Sci* 2004, 92, 3422.
21. Liang, R.; Liu, M. Z. *J Agric Food Chem* 2006, 54, 1392.
22. Guo, M.; Liu, M.; Zhan, F.; Wu, L. *Ind Eng Chem Res* 2005, 44, 4206.
23. *Humic Substances II: In Search of Structure*; Hayes, M. H. B.; MacCarthy, P.; Malcolm, R. L.; Swift, R. S., Eds.; Wiley: Chichester, England, 1989.
24. Russell, E. W. *Soil Conditions and Plant Growth*, 10th ed.; Longman: London, 1973.
25. Zhang, J. P.; Li, A.; Wang, A. Q. *React Funct Polym* 2006, 66, 747.
26. Zhang, J.; Yuan, K.; Wang, Y. P.; Gu, S. J.; Zhang, S. T. *Mater Lett* 2007, 61, 316.
27. Li, A.; Zhang, J. P.; Wang, A. Q. *Polym Adv Technol* 2005, 16, 675.
28. Zhang, J. P.; Liu, R. F.; Li, A.; Wang, A. Q. *Ind Eng Chem Res* 2006, 45, 48.
29. Wang, A. Q.; Zhang, J. P. *Organic-Inorganic Superabsorbent Composite*; Science: Beijing, 2006.
30. Chu, M.; Zhu, S. Q.; Li, H. M.; Huang, Z. B.; Li, S. Q. *J Appl Polym Sci* 2006, 102, 5137.
31. Liu, Z.; Zhou, P.; Yan, D. *J Appl Polym Sci* 2004, 91, 1834.
32. Zhang, J. P.; Chen, H.; Wang, A. Q. *Eur Polym J* 2006, 42, 101.
33. Zhang, J.; Chen, H.; Li, P.; Wang, A. *Macromol Mater Eng* 2006, 291, 1529.
34. Hooper, H. H.; Baker, J. P.; Blanch, H. W.; Prausnitz, J. M. *Macromolecules* 1990, 23, 1096.
35. Kiatkamjornwong, S.; Phunchareon, P. *J Appl Polym Sci* 1999, 72, 1349.
36. Hermans, J. J. *Flow Properties of Disperse System*; Wiley-Interscience: New York, 1953.
37. Zhang, J. P.; Chen, H.; Wang, A. Q. *Eur Polym J* 2005, 41, 2434.